

# Density of States of Landau Levels in Two-Dimensional Systems from Activated Transport, Magnetocapacitance and Gate Current Experiments

*D. Weiss\* and K. v. Klitzing*

Max-Planck-Institut für Festkörperforschung,  
D-7000 Stuttgart 80, Fed. Rep. of Germany

In this publication we demonstrate that a combination of capacitance and gate current experiments together with an analysis of thermally activated conductivity seems to be useful for the determination of the density of states (DOS) of Landau levels in two-dimensional systems. The experimental results suggest a Landau level width not far away from the predictions of the self-consistent Born approximation (SCBA) if the Fermi level is close to the center of a Landau level. The DOS between Landau levels however cannot be explained with such a narrow linewidth and the experiments suggest the existence of a background DOS or an increased linewidth broadening for integer filling factors.

## 1. Introduction

A microscopic theory of the quantum hall effect should give a correct description not only of the quantized resistivity values  $\rho_{xy} = h/ie^2$  but also of the transitions between the plateaus and the values of the finite resistivity  $\rho_{xx}$ . Such transport calculations are extremely complicated since the theory itself is complicated and in addition not enough information is available about the scattering centers. The published theories are based on certain approximations and assumptions about the distribution, the strength and the range of the scattering potential. A first test whether such assumptions are realistic should be available from a comparison between the calculated and the measured density of states  $D(E)$  since calculations of  $D(E)$  are much easier than a transport theory for  $\rho_{xx}(B)$  which includes complicated phenomena like localization and correlation. One of the first theories of the density of states (DOS) assumed short-range scatterers which leads within the self-consistent Born approximation (SCBA) to a broadening of the discrete energy spectrum (expected for an ideal two-dimensional electron gas without scattering) into an elliptic lineshape for the DOS [1]. Higher order approximations show that an exponentially decaying DOS is expected for energies  $E - E_n$  larger than the linewidth of the Landau levels  $E_n$  [2], so that a real energy gap with vanishing DOS may not be present but the DOS at midpoint between two Landau levels should decrease drastically if the magnetic field (energy separation between adjacent Landau levels) is increased. Experimental information about the DOS can be obtained from measurements of the specific heat [3], from magnetization measurements [4], from temperature-dependent resistivity measurements in the regime of the Hall plateaus [5], from magnetocapacitance measurements [6,7] or from gate current measurements [8]. In this article we compare the results we have obtained from an analysis of the thermally activated resistivity, magnetocapacitance and gate current measurements carried out on one and the same sample. The following discussion is based on a picture which does not include many-body effects. The notation "density of states (DOS)" in this paper is used to characterize the electronic properties within a single particle picture. All experiments described in the following have been carried out on AlGaAs-GaAs heterostructures.

## 2. Activated resistivity

The temperature dependence of  $\rho_{XX}^{\min}$  (where  $\rho_{XX}^{\min}$  means the minimum in the resistivity which corresponds to a Fermi level position very close to the midpoint between two Landau levels) in the temperature range  $2K < T < 20K$  is usually dominated by an exponential term corresponding to

$$\rho_{XX}^{\min} \sim \exp\left\{-\frac{E_{a,\max}}{kT}\right\}, \quad (1)$$

where  $E_{a,\max}$  denotes the measured activation energy. Measured activation energies  $E_{a,\max}$  for different samples at different magnetic field values are shown in Fig.1. The filling factor  $\nu$ , defined as  $\nu = n_s \frac{h}{eB}$  corresponds always to a fully occupied lowest Landau level ( $\nu=4$  for (100) silicon MOSFETs and  $\nu=2$  for GaAs-AlGaAs heterostructures). Since the measured activation energy  $E_{a,\max}$  agrees fairly well with half of the cyclotron energy  $\hbar\omega_c$ , this activation energy is interpreted as the energy difference between the Fermi energy  $E_F$  and the center of the Landau level  $E_n$ . For the sake of simplicity we assume that the mobility edge of the Landau level is located at the center of the Landau level, in agreement with calculations of the localization length [9] and percolation theories [10]. Furthermore the mobility edge is assumed to remain fixed, independent of the temperature and the carrier density. Changing the position of a Landau level  $E_n$  relative to the Fermi energy  $E_F$  (by changing the magnetic field) results in a reduced activation energy  $E_a = |E_n - E_F|$ . This motion of the Landau levels relative to the Fermi level if the filling factor of the Landau levels is varied is clearly visible in Fig.2. A change of the filling factor corresponds to a shift of the Fermi level, equivalent to a change  $\Delta n$  in the carrier density at fixed magnetic field. Measuring now the activation energy as a function of the magnetic field allows us to deduce a mean value for the DOS:

$$D(E) \approx \frac{\Delta n}{\Delta E}, \quad (2)$$

where  $\Delta E$  is the energy difference between activation energies determined at consecutive magnetic field values. This analysing technique is restricted to the tails of Landau levels and has been described in more detail in a previous publication [8]. Figure 3 shows the reconstructed DOS obtained from sample 1 ( $n_s = 2.60 \cdot 10^{11} \text{cm}^{-2}$ ,  $\mu = 158,000 \text{cm}^2/\text{Vs}$ ).

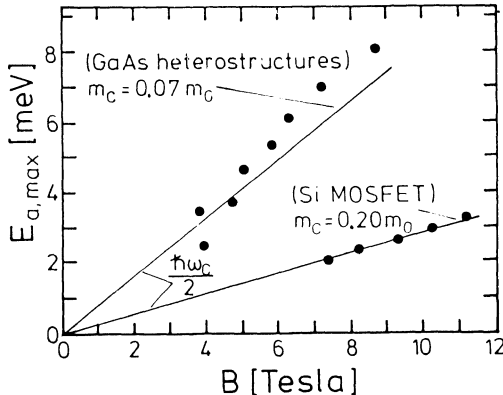


Fig. 1:

Measured activation energies  $E_{a,\max}$  in the resistivity at a filling factor corresponding to a fully occupied lowest Landau level as a function of the magnetic field  $B$ . The solid lines correspond to half of the cyclotron energy.

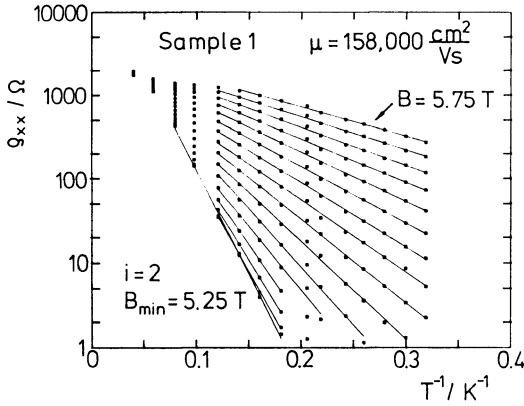


Fig. 2:

Temperature dependence of the resistivity  $\rho_{xx}$  at different magnetic fields close to a filling factor  $i=2$ .

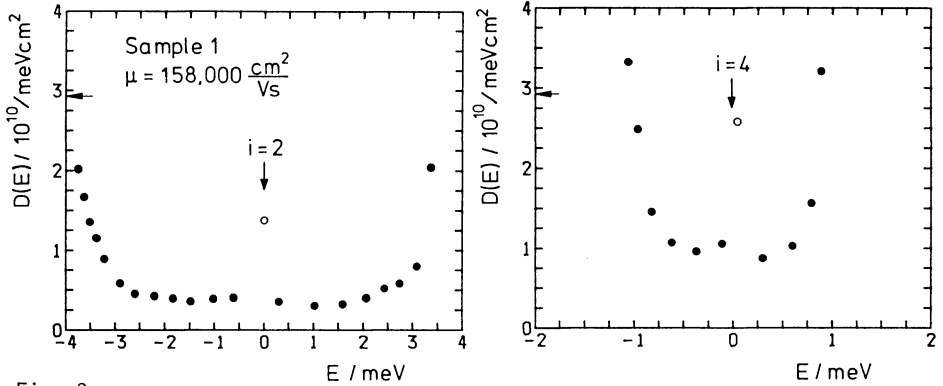


Fig. 3:

Reconstructed DOS for filling factors close to  $i=2$  and  $i=4$ . The arrow marks the zero magnetic field DOS. The energy scale is taken relative to the midpoint between two Landau levels

The DOS between Landau levels does not vanish but shows a value depending on the mobility of the sample and on the magnetic field. Decreasing mobility and decreasing magnetic field results in an increased DOS between Landau levels. The magnetic field dependence of the DOS between Landau levels - obtained from an analysis at filling factors close to  $i=2$  and  $i=4$  - is contrary to our previous statements. The high DOS close to  $E=0$  (Fig. 3) is an artefact of the analysis since for a Fermi energy at  $E=0$  two Landau levels contribute to  $\rho_{xx}$ . The reconstruction of the DOS from activated resistivity measurements is restricted to the tails of the Landau levels as mentioned above. Information about the DOS for a Fermi level position close to the center of a Landau level can be obtained from magnetocapacitance measurements described in the next chapter.

### 3. Magnetocapacitance

The capacitance experiments were carried out on gated GaAs-AlGaAs heterostructures with a Hall geometry. The mobilities of the samples described here are between 83,000 and 480,000  $\text{cm}^2/\text{Vs}$  for carrier densities in the

range between  $2.27 \cdot 10^{11} \text{cm}^{-2}$  and  $2.90 \cdot 10^{11} \text{cm}^{-2}$ . For capacitance measurements all the potential probes were short-circuited and acted as a channel contact.

The signal was obtained by measuring phase sensitive the voltage drop between the sample and a high-precision reference capacitor  $C_{\text{ref}}$  (see Fig. 4b). The signal  $V_{\text{meas}}$  is proportional to the capacitance difference  $C_{\text{sample}} - C_{\text{ref}}$  as long as the channel resistance  $R_{\text{ch}}$  is small compared to the AC resistance of  $C_{\text{sample}}$ . For a Fermi level position between two Landau levels  $\sigma_{xx}$  goes to zero and the signal  $V_{\text{meas}}$  is not directly proportional to the capacitance of the system but is influenced by the low conductivity state of the channel.

The capacitance of a system consisting of a metal-insulator-(with ionized impurities) semiconductor-sandwich (e.g. Au-AlGaAs-GaAs-heterostructure) depends not only on the thickness of the insulator but also on the DOS at the semiconductor side and on parameters of the material. Fig.4a shows the band diagram of a heterostructure including a Schottky gate in contact with the AlGaAs. If the two depletion layers interpenetrate each other the total capacitance at a given magnetic field can be expressed as [8,11]:

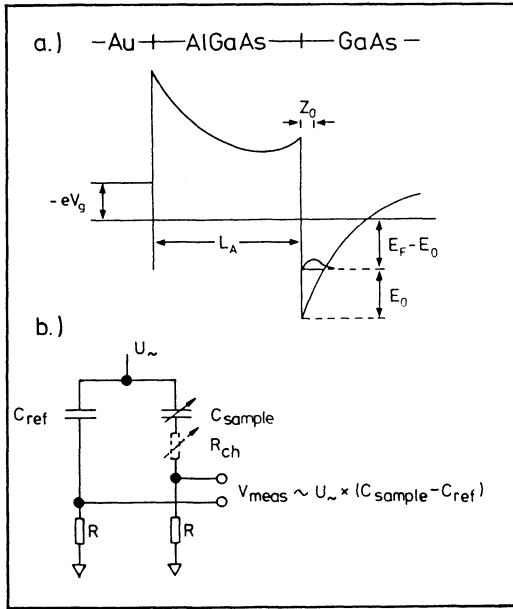


Fig. 4: Schematic diagrams of the conduction band edge for a gated GaAs-AlGaAs heterostructure showing the quantities used in the derivations (a) and the experimental set up (b).  $U_{\sim}$  is the AC component of the applied voltage with an amplitude of about 7 mV and a frequency of 223 Hz

$$\frac{1}{C} = \frac{1}{C_A} + \frac{\gamma z_0}{\epsilon_S} + \frac{1}{e^2} \frac{dn_s}{d(E_F - E_0)} \Big|_{E_F} \quad (3)$$

where  $C_A$  is the capacitance of the insulating AlGaAs layer,  $\epsilon_S$  is the dielectric constant of GaAs,  $z_0$  is the average position of the electrons in the channel,  $\gamma$  is a constant numerical factor between 0.5 and 0.7, and  $dn_s/d(E_F - E_0)$  is the thermodynamic DOS at the Fermi level, in the following denoted as  $dn_s/dE_F$ . The first two terms on the right-hand side of (3) are

assumed to be constant in a magnetic field, and thus changes of the capacitance are directly related to changes in the thermodynamic DOS of the 2DEG. At  $T=0$  the total inverse capacitance in a magnetic field can be expressed as

$$\frac{1}{C} = \frac{1}{C_0} - \frac{1}{e^2 D_0} + \frac{1}{e^2 D} \quad , \quad (4)$$

where  $C_0$  denotes the value of the total capacitance at  $B=0$ ,  $D$  is the DOS at the Fermi level in the presence of a magnetic field and  $D_0$  is the DOS within the lowest subband, equal to  $2.9 \times 10^{10} \text{cm}^{-2} \text{meV}^{-1}$  in the absence of a magnetic field. At finite temperatures  $D$  has to be replaced by  $dn_S/dE_F$ .

The experimental results were compared with calculations of  $C(B)$  assuming a Gaussian-like DOS of the form:

$$D(E) = \frac{e}{\pi \hbar} \cdot \frac{1}{\sqrt{2\pi}} \cdot \frac{B}{T} \cdot \sum_n \exp\left\{-\frac{(E - (n+\frac{1}{2}) \hbar \omega_C)^2}{2\Gamma^2}\right\} \quad , \quad (5)$$

where  $\Gamma$  is the broadening parameter of the Gaussian distribution. First the position of the Fermi level  $E_F$  is determined by solving numerically the equation:

$$n_S = \int_{-\infty}^{\infty} D(E) f(E - E_F) dE \quad , \quad (6)$$

where  $f(E - E_F)$  is the Fermi distribution function. The carrier density  $n_S$  is assumed to be independent of magnetic field and temperature.

In the next step the thermodynamic DOS

$$\left. \frac{dn_S}{dE_F} \right|_{E_F} = \int_{-\infty}^{\infty} D(E) \cdot \left. \frac{df(E - E_F)}{dE_F} \right|_{E_F} dE \quad (7)$$

is calculated numerically. With the temperature-dependent form of (4) and (7) one obtains  $C(B)$ . Spin splitting which is small compared to the cyclotron energy for GaAs is neglected in the calculations.

Fig. 5 shows the capacitance data (for the same sample as discussed in Fig. 3) at different temperatures together with a theoretical curve calculated on the basis of a magnetic field independent linewidth  $\Gamma=0.48$  meV. We have adjusted the fit to the magnetocapacitance maxima since the observed minima may be falsified - at least at high magnetic fields and low temperatures - by the small channel conductance. This argument cannot be used to explain the reduced depth of the capacitance minima at magnetic fields below 2 Tesla since the phase shift due to the channel resistance is negligibly small. However, inhomogeneities may explain the experimental data as shown in Fig. 6 where the change in the capacitance due to a Gaussian distribution of the carrier density  $n_S$  with a broadening parameter  $\Delta n_S=0.015 n_S$  is shown. A remarkable reduction of the depth of the capacitance minima is visible whereas the maxima remain unchanged.

The influence of inhomogeneities has been considered in a more sophisticated way by Gerhardt and Gudmundsson [12] in their statistical model for inhomogeneities. Their model is based on the assumption of a Gaussian-shaped DOS and the result of the calculations can be described using an effective linewidth  $\Gamma$  shown in Fig. 7. This effective linewidth oscillates and a maximum is always obtained for a Fermi level position between two

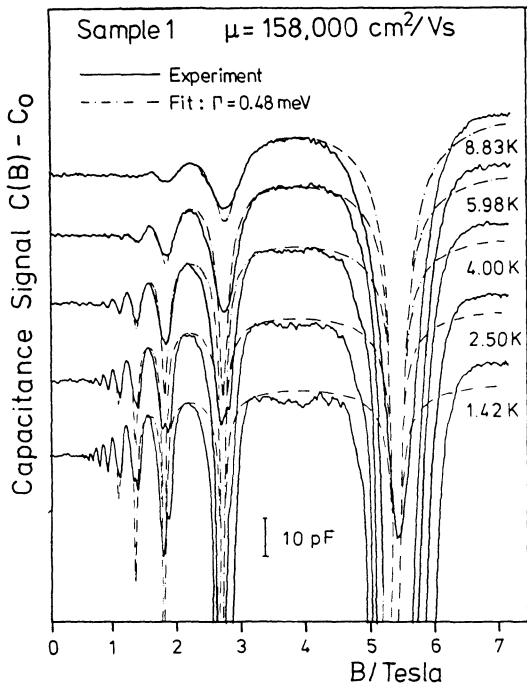


Fig. 5:  
 Measured magnetocapacitance and corresponding fit using a broadening parameter  $\Gamma = 0.48 \text{ meV}$  in the model DUS. For the sake of clarity the curves are shifted vertically

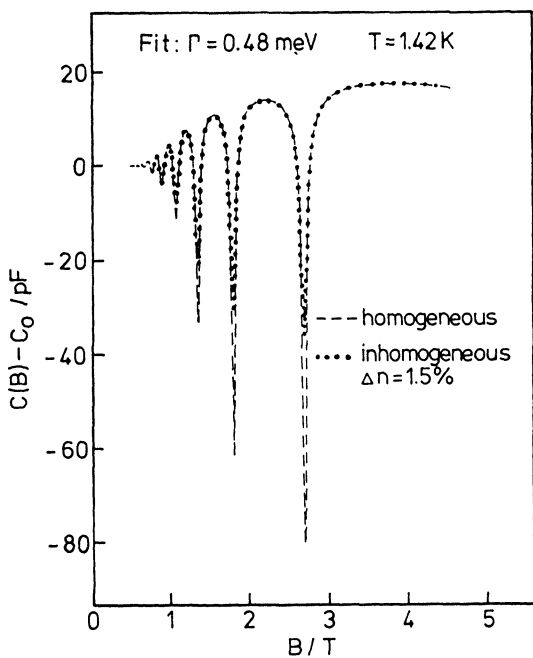


Fig. 6:  
 Calculated magnetocapacitance showing the influence of inhomogeneities assuming a Gaussian distribution of the carrier density  $n_s$

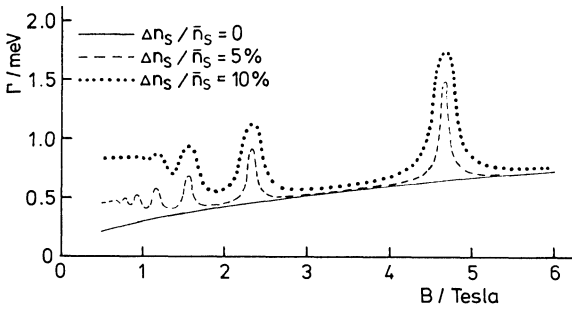


Fig. 7:  
Effective Landau level  
broadening as a function  
of B. After [13]

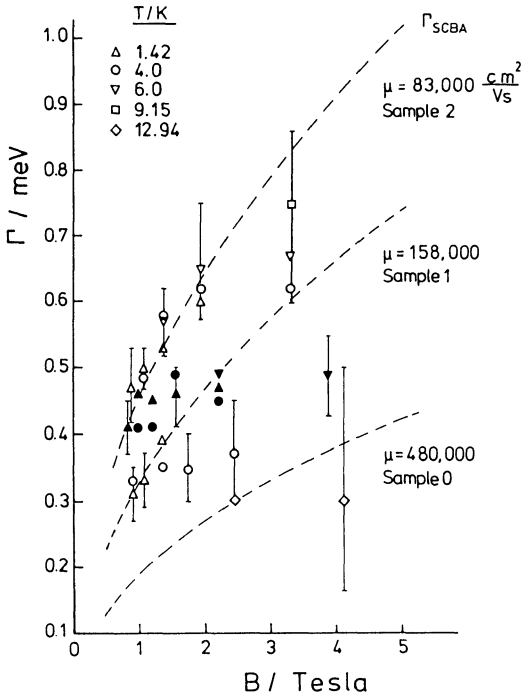


Fig. 8:  
Landau level width  $\Gamma$  vs. B.  
Points are obtained by compar-  
ing magnetocapacitance maxima  
with model calculations. The  
dashed line corresponds to the  
SCBA- linewidth (8) where  $\mu$  is  
the mobility of the samples.  
Full symbols correspond to  
sample 1 and lie in the range  
between open symbols corres-  
ponding to sample 0 and  
sample 2

Landau levels. This aspect is similar to calculations of the oscillating level broadening due to screening effects [14-16].

Figure 8 summarizes the results obtained from an analysis of the magnetocapacitance maxima of three samples. In this figure the broadening parameter  $\Gamma$  (see (5)) is plotted as a function of the magnetic field and compared with the linewidth  $\Gamma_{SCBA}$ , obtained from the selfconsistent Born approximation (SCBA) [1]:

$$\Gamma_{SCBA} = \frac{eh}{m^*} \sqrt{\frac{2}{\pi} \cdot \frac{B}{\mu}} \quad (8)$$

where  $m^*$  is the effective mass and  $\mu$  the mobility of the sample. Fitting the magnetocapacitance maxima means that each point in Fig. 8 corresponds

to a Fermi level position close to the center of a Landau level. The linewidth has been extracted from measurements at different temperatures indicated by different symbols. Figure 8 shows that the experimentally deduced linewidths are not so far away from the predictions of the SCBA - the  $\sqrt{B}$  dependence of the linewidth  $\Gamma$  is more or less visible for the sample with the lowest mobility.

Up to now the model calculation of the magnetocapacitance was based on the assumption that the carrier density in the channel remains constant. This is incorrect, since the difference in the electrochemical potential across the capacitor is fixed and a variation in the capacitance leads to a charge transfer between the gate electrode and the channel. This small change in the carrier density is unimportant in an analysis of capacitance measurements but is a first order contribution in gate current experiments which will be discussed in the following chapter.

#### 4. Gate Current

The assumption that the carrier density  $n_s$  remains constant changing the magnetic field is not correct. Actually not the carrier density  $n_s$  but the Fermi level is kept constant during capacitance experiments. Using the notation of Fig. 4a this means that the gate voltage  $V_g$  is kept constant. Varying the magnetic field  $B$  then leads to oscillations of the surface potential (bottom of the potential well) and to a charge transfer between gate and channel of the heterostructure. Since the amount of transferred charge is small compared to the two-dimensional carrier density  $n_s$  the subband edge (taken relative to the bottom of the potential well) is assumed to be constant. The starting point for the model calculations is now no longer (5) but the following equation [8]:

$$\int_{-\infty}^{\infty} D(E) f(E - E_F) dE + \frac{C_A}{e^2} E_F = \text{const} , \quad (9)$$

where the constant can be determined at  $B=0$ . Equation (9) has to be solved numerically to give the correct position of the subband edge relative to the Fermi level and then the magnetocapacitance can be calculated using (7) and the temperature dependent form of (4). Calculating the magnetocapacitance in the way described above results in a broadening of the width of the capacitance minima compared to calculations assuming a constant carrier density  $n_s$ . The difference however is small and cannot be resolved in Fig. 5. The charge flow mentioned above can be determined by measuring the current between gate and channel as a function of the magnetic field  $B$ . The current flow is given by

$$I(B) = A \cdot e \cdot \frac{dn_s}{dt} = A \cdot e \cdot \frac{dn_s}{dB} \cdot \frac{dB}{dt} , \quad (10)$$

where  $A$  is the area of the two-dimensional electron gas and  $dB/dt$  the sweep rate of the magnetic field.  $dn_s/dB$  can be determined by solving (9) at different magnetic fields since the first term on the left-hand side is equal to the carrier density  $n_s$ . The current flow versus magnetic field is shown in Fig. 9. The upper curve shows the experiments (carried out again on sample 1) where a current minimum corresponds to a DOS maximum and a maximum in the current flow corresponds to a Fermi level position in a minimum of the DOS. The origin of the reverse current peak at about 5.2 Tesla is not clear yet. The experiment is compared with model calculations using a Landau level linewidth (gaussian) of  $\Gamma = 0.48$  meV (see Fig. 5 and Fig. 8) and 1.35 meV. The smaller linewidth  $\Gamma = 0.48$  meV obtained from an



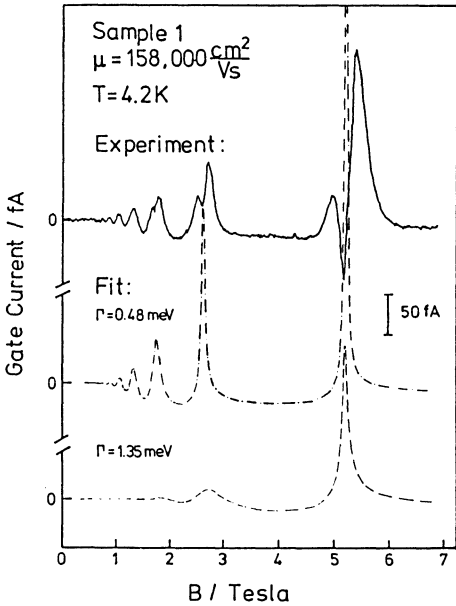


Fig. 9:  
 Measured and calculated current flow between gate and channel of sample 1 vs. magnetic field

analysis of the magnetocapacitance maxima of the same sample - again describes correctly the experiment for a Fermi level position close to the center of a Landau level. A larger linewidth  $\Gamma = 1.35 \text{ meV}$  cannot fit the oscillations at lower magnetic field but fits approximately the height of the measured current maximum at about 5.4 Tesla (filling factor  $i \approx 2$ ).

A more quantitative analysis however is hindered by the reverse current peak. It should be noted that the statistical model [12,13] or a background DOS at  $i=2$  produces more broadened current maxima, comparable to the experimental ones.

## 5. Summary

Three different experimental methods have been carried out on one and the same sample. These three methods are sensitive to different energetical regions of the DOS. An analysis of the thermally activated resistivity - restricted to the tails of the Landau levels - shows a nonvanishing DOS between Landau levels depending on mobility and magnetic field which cannot be explained within the SCBA or higher order approximations. Magnetocapacitance measurements however are mainly restricted to the maxima of the DOS.

If the Fermi level position is close to the center of a Landau level the magnetocapacitance data can be explained with a Gaussian-shaped DOS where the linewidth  $\Gamma$  follows roughly the SCBA predictions. Gate current experiments in principle are sensitive to maxima as well as to minima in the DOS. For a Fermi level position in a maximum of the DOS the gate current measurements show the same result as magnetocapacitance measurements. The explanation of the gate current measurements for a Fermi level position between two Landau levels requires a background DOS or an increased linewidth broadening.

## Acknowledgement

We would like to thank R. Gerhardt and V. Gudmundsson for stimulating discussions and their interest in this work. We are grateful to K. Ploog and G. Weimann for providing the samples and we appreciate the cooperation with E. Stahl and V. Mosser at earlier stages of this work.

## References

\* Present address: Physik-Department E16, Technische Universität München, D-8046 Garching

1. T. Ando, Y. Uemura: J.Phys.Soc.Jap. 36, 959 (1974)
2. R.R. Gerhardt: Surf.Sci. 58, 227 (1976)
3. E. Gornik, R. Lassnig, G. Strasser, H.L. Störmer, A.C. Gossard, W. Wiegmann: Phys.Rev.Lett. 54, 1820 (1985)
4. J.P. Eisenstein, H.L. Störmer, V. Narayanamurti, A.Y. Cho, A.C. Gossard: Phys.Rev.Lett. 55, 875 (1985)
5. E. Stahl, D. Weiss, G. Weimann, K. v.Klitzing, K. Ploog: J.Phys. C18, L783 (1985)
6. T.P. Smith, B.B. Goldberg, P.J. Stiles, M. Heiblum: Phys.Rev. B32, 2696 (1985)
7. V. Mosser, D. Weiss, K. v.Klitzing, K. Ploog, G. Weimann: Solid State Commun. 58, 5 (1986)
8. D. Weiss, K. v. Klitzing, V. Mosser: in Two-Dimensional Systems: Physics and New Devices, ed. by G. Bauer, F. Kuchar, H. Heinrich, Springer Ser. Solid State Sci., Vol. 67 (Springer, Berlin, Heidelberg 1986) p. 204
9. T. Ando: J.Phys.Soc.Jap. 53, 3101 (1984)
10. S.A. Trugman: Phys.Rev. B27, 7539 (1983)
11. F. Stern: Phys.Rev. B5, 4891 (1972)
12. R.R. Gerhardt, V. Gudmundsson: Phys.Rev. B34, 2999 (1986)
13. V. Gudmundsson, R.R. Gerhardt: to be published
14. R. Lassnig, E. Gornik: Solid State Commun. 47, 959 (1983)
15. T. Ando, Y. Murayama: J.Phys.Soc. Japan. 54, 1519 (1985)
16. W. Cai, T.S. Ting: Phys.Rev. B33, 3967 (1986)